Optimum HI to H_2 Conversion

1

Numerical Simulations of HI Decomposition in Packed Bed Membrane Reactor with Molten Salt Heating

B. C. Nailwal[1], N. Goswami[1]*, Soumitra Kar[1, 2] and A. K. Adak[1]

[1]*Desalination & Membrane Technology Division, Bhabha Atomic Research Centre (BARC), Trombay – 400085, INDIA*
[2]*Homi Bhabha National Institute, Anushaktinagar, Mumbai- 400094, INDIA*

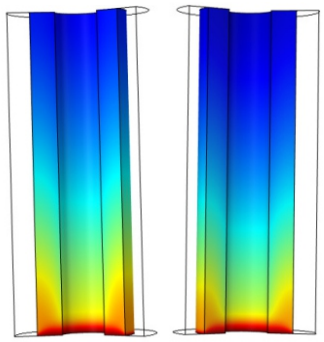

HI mole fraction profile inside the membrane reactor at different outlet pressures

ABSTRACT

Hydrogen is considered amongst clean fuel options, for its utilization does not lead to emission of any pollutant or greenhouse gases. Water electrolysis and thermochemical cycles, coupled with renewable or nuclear energy source, are two important processes for green hydrogen energy production. Amongst the thermochemical routes, Iodine-Sulfur (IS) cycle offers advantages of higher efficiency and no solid handling. Efficiency of HI_x processing section dictates the overall efficiency of IS thermochemical cycle. This section handles highly corrosive species, while the HI to H_2 equilibrium conversion is very low (~22%) at 700 K. In this work, the authors have carried out simulations of single-tube membrane reactor using tantalum composite membrane, coupled with molten salt heating, to determine the effect of various operating parameters on the conversion of HI. The optimum molten salt inlet temperature is found to be ~773 K, as beyond this temperature the conversion of HI does not increase, posing in addition the materials challenges. The findings confirmed that at a feed velocity of 0.0005 m/s, a conversion of ~83% can be achieved with the membrane tube radius of ~36 mm and a pressure of 3 bar. The studies provide useful insights into a molten-salt heated membrane reactor for optimum HI to H_2 conversion.

KEYWORDS: *Green hydrogen energy, Iodine-Sulfur (IS) cycle, Membrane reactor*

Introduction

It is important to reduce dependency on fossil fuels and look for promising alternatives. As energy demands are going to increase due to industrialization, population growth and betterment of life standards, the new technologies must be expandable. The upcoming energy sources needs to be environment friendly, i.e., energy sources should be green and cost effective. Considering these factors, hydrogen energy economy is going to be a game changer, offering a clean and green source of energy. Amongst different hydrogen production methods, steam reforming and water electrolysis are proven and used extensively for the production of hydrogen today. Thermochemical cycles have definite advantage over the electrochemical process because they do not involve conversion of heat into electricity. The IS cycle, a closed-loop thermochemical water splitting process, is of particular interest because unlike contemporary methods, it can produce hydrogen efficiently in being coupled with nuclear/solar energy source.

Following reactions are involved in IS process:

$$I_2 + SO_2 + 2H_2O \rightarrow 2HI + H_2SO_4 \text{ (Bunsen reaction)} \quad (1)$$

$$H_2SO_4 \rightleftharpoons H_2O + SO_2 + 0.5O_2 \quad (2)$$

$$2HI \rightleftharpoons H_2 + I_2 \quad (3)$$

In Bunsen reaction (first reaction), H_2O reacts with I_2 and SO_2 to produce HI and H_2SO_4. In the second reaction, decomposition of H_2SO_4 to O_2, SO_2 and H_2O takes place, and SO_2 is recycled back to the Bunsen reaction. In the third reaction, decomposition of HI to H_2 and I_2 occurs. H_2 is collected as the product and I_2 is recycled back to the Bunsen section. The overall reaction is decomposition of H_2O into H_2 and O_2 [1]. However, the IS process has got several challenges.

The decomposition of HI to hydrogen is an equilibrium limited reaction with a very low conversion [2], leading to reduction in overall thermal efficiency of the process. In order to address this, ongoing research is focussed on development of membrane reactor [3]. In this work, CFD simulations of packed bed membrane reactor for HI decomposition using molten salt heating have been carried out. The molten salt is an effective technique to couple membrane reactor heating requirement with solar/nuclear energy. In this work, molten nitrate salt has been considered as the heating medium. Fig.1 shows the schematic of molten salt heated packed bed membrane reactor setup.

In this work, to the best of authors' knowledge, simulation studies on molten salt heated tantalum membrane-based reactor for application in IS thermochemical process are being reported for the first time.

Computational Approach

Momentum Transport

For packed bed membrane reactor Brinkman equation (Eq. (1)) was used.

$$\frac{\eta}{K}\vec{u} + \nabla.\left[pI - \frac{\eta}{\varepsilon}\left(\nabla\vec{u} + (\nabla\vec{u})^T\right)\right] = 0 \quad (1)$$

*Author for Correspondence: Nitesh Goswami
E-mail: niteshg@barc.gov.in

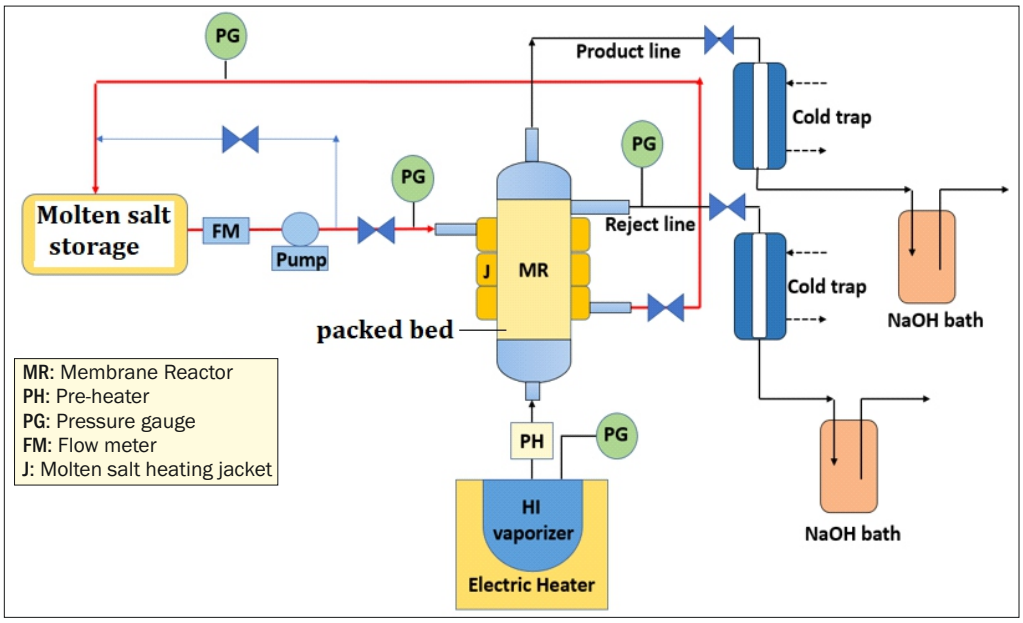

Fig.1: Schematic of molten salt heated packed bed membrane reactor setup.

The hydraulic permeability (κ) of the porous medium is defined by Eq. (2).

$$K = \frac{(d_p)^2 \varepsilon^3}{180(1-\varepsilon)^2} \quad (2)$$

To model momentum transport for molten salt flow in the jacket, Navier-Stokes equation was used.

Energy Transport

Eq. (3) is the energy transport equation used in the modelling. This equation has been used for simulation of both membrane reactor and molten salt heating domain. The equation accounts for both convective and conductive transport of the heat as well as heat generation due to reaction.

$$\rho C_p \left(\frac{\partial T}{\partial t} + \vec{u}.\nabla T\right) = \nabla.(k_t \nabla T) + Q \quad (3)$$

For molten salt heating, Q is taken as zero.

Species Transport

For species transport, Maxwell-Stefan diffusion and convection equation (Eq. (4)) was used for HI, H_2 and I_2.

$$\nabla.\left((\rho\omega_i\vec{u} - \rho\omega_i \sum_{j=1}^{n} D_{ij}(\nabla x_j + (x_j - \omega_j)\frac{\nabla p}{p}\right) - D_i^T \frac{\nabla T}{T}) = R_i \quad (4)$$

Reaction Kinetics

Langmuir-Hinshelwood type rate equation, as proposed by Oosawa et al [4] was used for carrying out the simulations. The simulations are carried out using the membrane permeability reported in literature [5]. The relevant expressions are given by Eqs. (5) – (8).

$$r_{HI} = - kpR_{HI} \quad (5)$$

$$R_{HI} = \frac{x_{HI}}{1+K_{I_2} p x_{I_2}} - \frac{\sqrt{x_{H_2} x_{I_2}}(1 + K_{I_2} p \frac{\Phi e}{2})}{K p (1 + K_{I_2} p x_{I_2})^2} \quad (6)$$

$$k = 1.58 \times 10^{-1} \exp\left(\frac{-34.31 \times 10^3 J\ mol^{-1}}{RT}\right) \quad (7)$$

$$K_{I2} = 5.086 \times 10^{-11} \exp\left(\frac{86.66 \times 10^3 J\ mol^{-1}}{RT}\right) \quad (8)$$

The equilibrium constant, K_p for the decomposition of HI was obtained by the free energy values (ΔG ~ 12 kJ/mol) given in the JANAF [6], by means of the following equation:

$$K_P = \exp\left(\frac{-\Delta G}{RT}\right) \quad (9)$$

The physical properties for all the species like heat capacity, viscosity, density and thermal conductivity were calculated using equations reported in our previous work [7]. All these physical properties were taken to be temperature and pressure dependent.

Boundary Conditions

Fig.2 shows the computational domain with boundary conditions. A membrane reactor with single membrane tube has been considered for simulations.

For Momentum Transport:

- Outlet pressure of membrane reactor: p_0
- Inlet feed velocity to membrane reactor: u_0
- At wall: No slip condition
- Inlet velocity of molten salt: 0.0005 m/s
- Outlet pressure of molten salt: 1 atm

For Energy Transport:

- Inlet feed temperature to membrane reactor: 523 K
- At outlet of membrane reactor: $k_t \nabla T = 0$, $q.\vec{n} = \rho C_p T\ \vec{u}$
- At molten salt wall: $Q_w = U\ A\ (T_2 - T)$
- Inlet temperature of molten salt: T_1

For Species Transport:

- Inlet mole fraction of HI, x_{10}: 0.95
- At outlet of the membrane reactor: $Di.\nabla ci = 0$, $N_i.\vec{n} = c_i u.\vec{n}$
- Flux of hydrogen at membrane wall: Pe p x_2

Validation of model

Since there is no relevant experimental data available in literature for the reactor geometry and conditions which have been used in the simulations of this work, an attempt was made to model a packed bed tubular reactor for steam

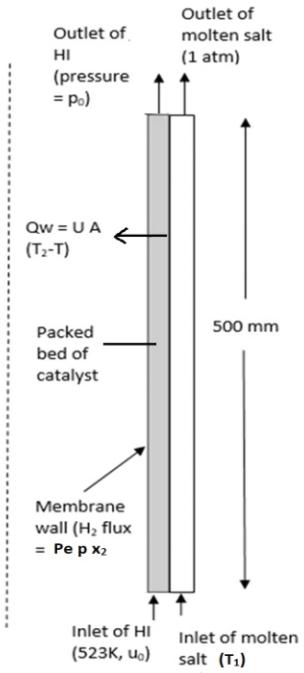

Fig.2: Computational domain with boundary conditions (dashed line show the axis of symmetry).

reforming of methanol using COMSOL Multiphysics by adopting the computational approach used for modeling of membrane reactor for HI decomposition in this study. The experimental data for steam reforming of methanol for packed bed tubular reactor has been reported in the literature [8]. The modeling of steam reforming of methanol was carried out to see the effect of ratio of weight of catalyst to methanol feed flow rate on the conversion. The results obtained by modeling were close to the values obtained through experiments. Table 1 shows the experimental and simulation results for the steam reforming of methanol (where X_{sim} is the conversion obtained by simulations and X_{exp} is the conversion reported in literature). The match between the experimental and simulation results for this case validates the computational approach which is then used for modeling of membrane reactor for HI decomposition in this work.

Results and Discussion

The computational approach validated with the reported experimental data of steam reforming of methanol was used to perform parametric analysis for HI decomposition reaction in molten salt heated single-tube membrane reactor. This section presents the results of this parametric analysis.

Effect of outlet pressure of reactor

Fig.3 shows the effect of pressure on conversion of HI inside the membrane reactor. It is observed that as the outlet pressure increases from 0.3 bar to 3 bar, the conversion of HI decomposition increases from 55% to 83%. It may be noted that the ceramic support tube on which metal is coated to fabricate the membrane can tolerate pressure up to 5 bar. As the pressure increases, the partial pressure of hydrogen increases due to increase in overall pressure leading to increase in driving force across the membrane for hydrogen transport. This increase in driving force leads to increase in flux of membrane as shown in Fig.4. The hydrogen flux increases from 3.15 x 10^{-7} kg/m^2.s to 4 x 10^{-6} kg/m^2.s as pressure is increased from 0.3 bar to 3 bar. Due to increase in hydrogen separation from the reaction mixture owing to permeation through the membrane, the HI decomposition reaction is pushed forward to a greater extent, leading to increased conversion.

Table 1: Validation of numerical simulations.

Ratio of catalyst mass to feed flow rate	X_{sim}	X_{exp}	Deviation (%)
35	0.959	0.89	7.7
40	0.967	0.9	7.4
45	0.972	0.92	5.6
50	0.976	0.94	3.8
55	0.979	0.95	3.1

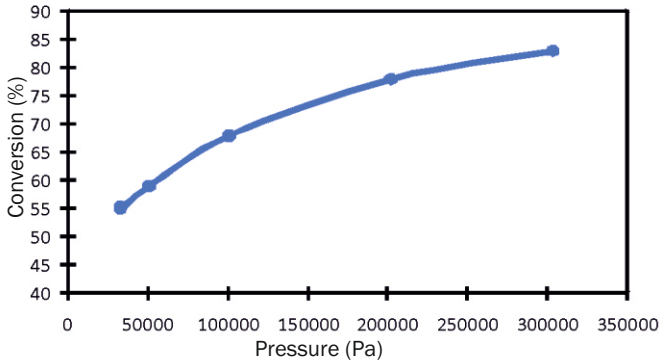

Fig.3: Effect of pressure on conversion of HI (u_0 = 0.0005 m/s, T_f = 500K, T_1= 823K, x_{10} = 0.95, ε = 0.3).

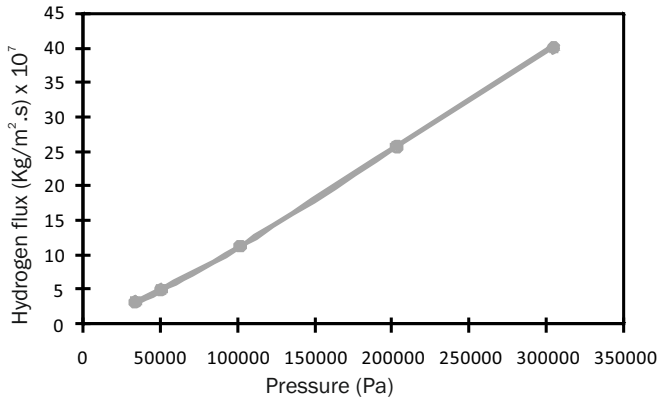

Fig.4: Effect of pressure on average flux of hydrogen (u_0 = 0.0005 m/s, T_f = 500K, T_1= 823K, x_{10} = 0.95, ε = 0.3).

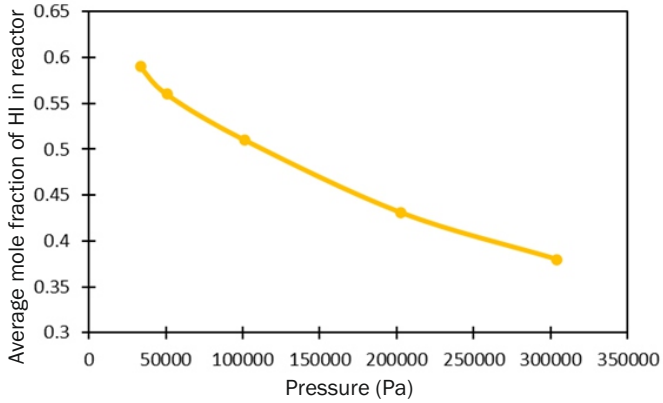

Fig.5: Effect of pressure on average mole fraction of HI in reactor (u_0 = 0.0005 m/s, T_f = 500K, T_1= 823K, x_{10} = 0.95, ε = 0.3).

Fig.5 shows the effect of pressure on the average mole fraction of HI inside the membrane reactor. It is observed that the average mole fraction of HI decreases from 0.59 to 0.38 with increase in pressure from 0.3 bar to 3 bar. As the pressure increases, the flux through membrane increases which leads to increase in decomposition of HI and reduction of average mole fraction of HI.

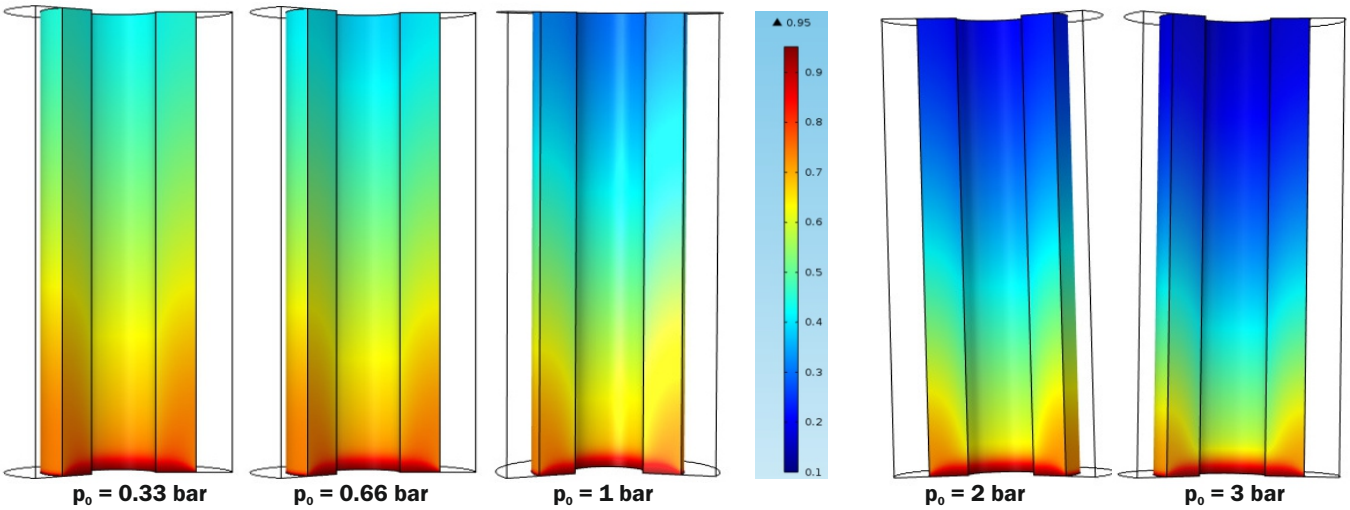

Fig.6: HI mole fraction profile inside the membrane reactor at different outlet pressures (u_0 = 0.0005 m/s, T_f = 500K, T_1 = 823K, x_{10} = 0.95, ε = 0.3).

Fig.6 shows the contours of mole fraction of HI inside the membrane reactor at different pressures. It is seen that at higher pressure, the mole fraction becomes constant after a small distance from the inlet. This shows reaction reaching equilibrium within a short distance from the inlet at higher pressures. At lower pressure, the mole fraction of hydrogen does not become constant in axial direction indicating reaction is taking place throughout the reactor. The mole fraction of HI was found to be lower close to the membrane wall of reactor. This is because hydrogen permeation is higher in this zone and hence conversion also increases which leads to increased decomposition of HI near the walls.

Effect of inlet temperature of molten salt

Fig.7 shows the effect of inlet temperature of molten salt on the conversion of HI to hydrogen. It is observed that with increase in molten salt inlet temperature from 623 K to 823 K, the conversion of HI increases from 39 to 83%. With increase in temperature, rate of the reaction increases hence the conversion increases. It is also observed that beyond a certain point, the conversion becomes almost constant and does not change with temperature. This is because after a certain point, the membrane surface area is not sufficient to remove the increased amount of hydrogen from the reaction zone, leading to saturation in conversion. At the same time, density of gas mixture decreases with increases in temperature which lowers the residence time of gases. This is also corroborated from results shown in Fig.8 in which it can be observed that the hydrogen flux becomes almost constant after temperature of 773 K. Hence, it can be concluded that increasing the temperature beyond 773 K is not useful for conversion enhancement.

Fig.9 shows the effect of inlet temperature of molten salt on hydrogen generation rate inside the membrane reactor. It can be observed that it increases with increase in molten salt inlet temperature. In this case also, it can be seen that beyond 773 K, the rate of increase in hydrogen generation rate decreases as conversion tends to stagnate due to reasons mentioned earlier.

Fig.10 shows the contours of mole fraction of HI inside the membrane reactor at different inlet temperatures of molten salt. It is seen that at higher temperature (beyond 773 K), the mole fraction becomes constant after a small distance from the inlet. This shows reaction reaching equilibrium within a short distance from the inlet at higher temperatures. At lower temperatures, the mole fraction of HI varies in axial direction throughout the reactor length indicating higher utilization of membrane reactor length.

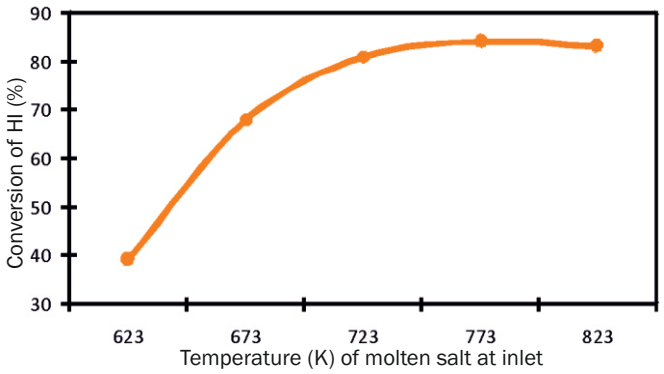

Fig.7: Effect of molten salt inlet temperature on HI conversion (u_0 = 0.0005 m/s, T_f = 500K, x_{10} = 0.95, ε = 0.3, p_0 = 303975 Pa).

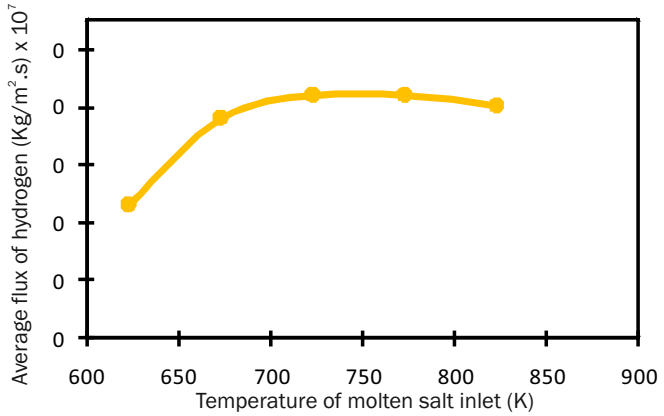

Fig.8: Effect of molten salt inlet temperature on average flux of H_2 (u_0 = 0.0005 m/s, T_f = 500K, x_{10} = 0.95, ε = 0.3, p_0 = 303975 Pa).

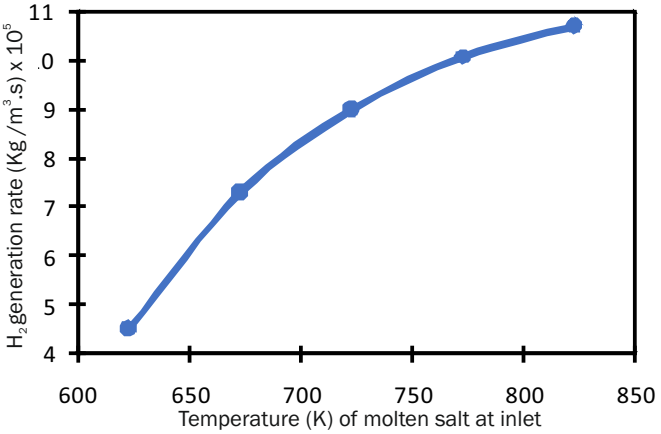

Fig.9: Effect of molten salt inlet temperature on H_2 generation rate (u_0 = 0.0005 m/s, T_f = 500K, x_{10} = 0.95, ε = 0.3, p_0 = 303975 Pa).

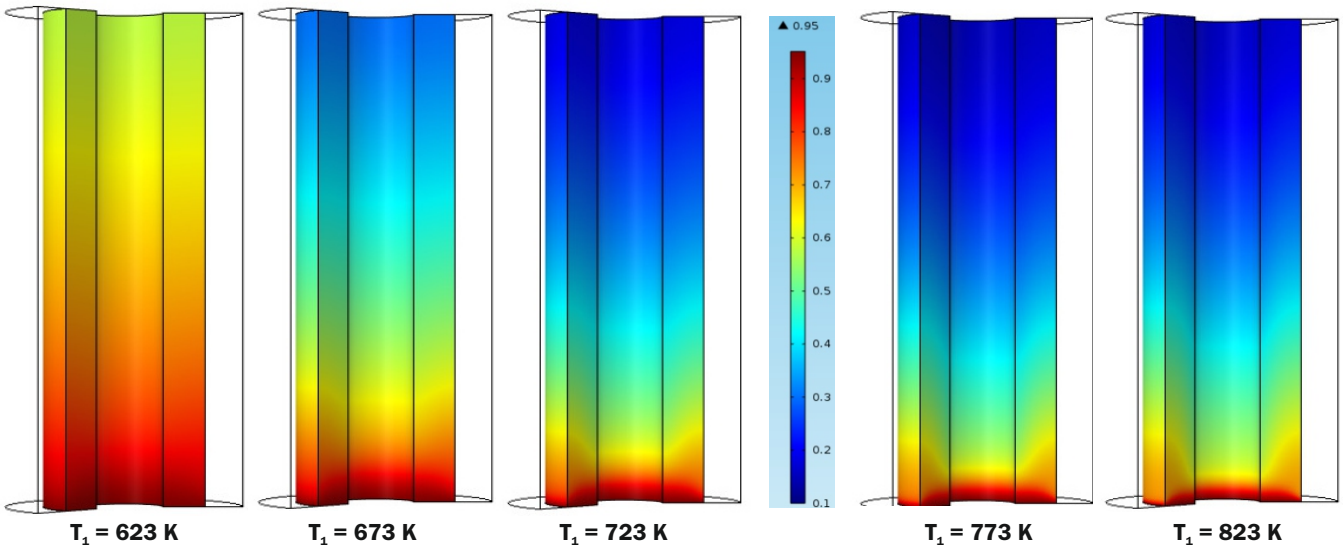

Fig.10: HI mole fraction profile inside the membrane reactor at different inlet temperatures of molten salt (u_0 = 0.0005 m/s, T_f = 500K, x_{10} = 0.95, ε = 0.3, p_0 = 303975 Pa).

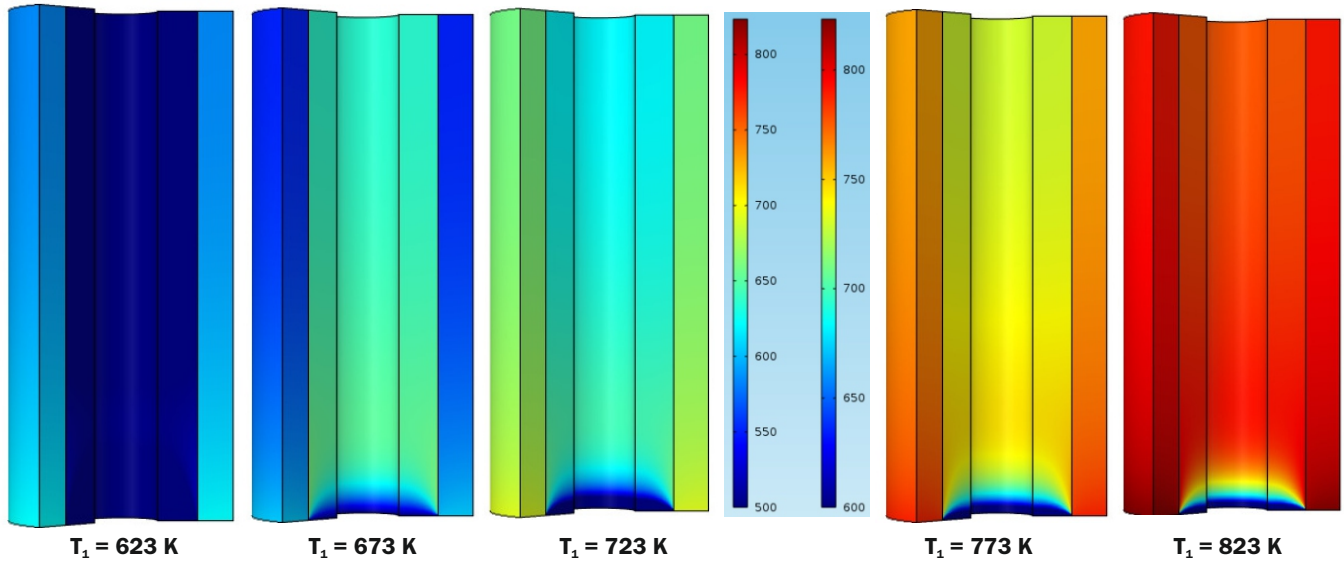

Fig.11: Contours of temperature inside the membrane reactor at different inlet temperatures of molten salt (u_0 = 0.0005 m/s, T_f = 500K, x_{10} = 0.95, ε = 0.3, p_0 = 303975 Pa; the first scale corresponds to reaction mixture temperature and the second corresponds to molten salt temperature).

Fig.11 shows the contours of temperature inside the membrane reactor and in the molten salt flow channel at different inlet temperatures of molten salt. It is seen that at all the values of molten salt inlet temperatures, the temperature inside the reactor becomes constant after a small distance from the inlet. Hence, it can be concluded that for the entire range of molten salt inlet temperatures, the temperature of the reactor remains uniform throughout. This is because this simulation is carried out at optimised feed velocity of 0.0005 m/s, at which the residence time of reactant species is sufficient to allow effective heat transfer causing the temperature to become constant within a short distance from inlet.

Effect of feed velocity

Fig. 12 shows the effect of feed velocity on conversion of HI. As the feed velocity increases, conversion reduces. A conversion of ~83% is obtained at a feed velocity of 0.0005 m/s. From this figure, it may be concluded that lower velocities increase the residence time and hence the conversion. So, it would be preferable to operate the reactor at a low feed rate, however, it will be at the cost of lower throughput.

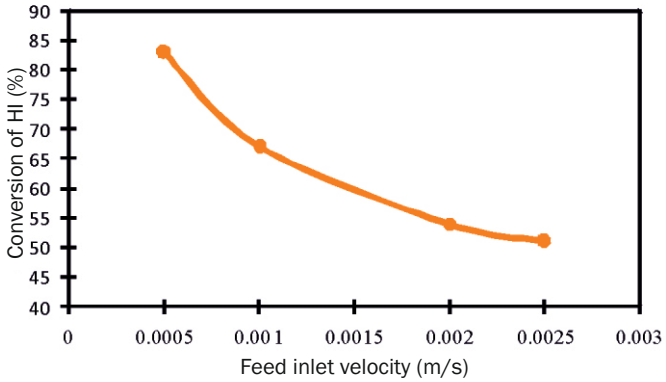

Fig.12: Effect of feed velocity on conversion of HI (T_1 = 773 K, T_f = 500K, x_{10} = 0.95, ε = 0.3, p_0 = 303975 Pa).

Effect of flow direction of molten salt

Fig.13 shows the conversion of HI decomposition inside the membrane reactor for co-current and counter-current flow of molten salt with respect to the feed flow. It is observed that a higher conversion of ~83% is achieved in co-current flow

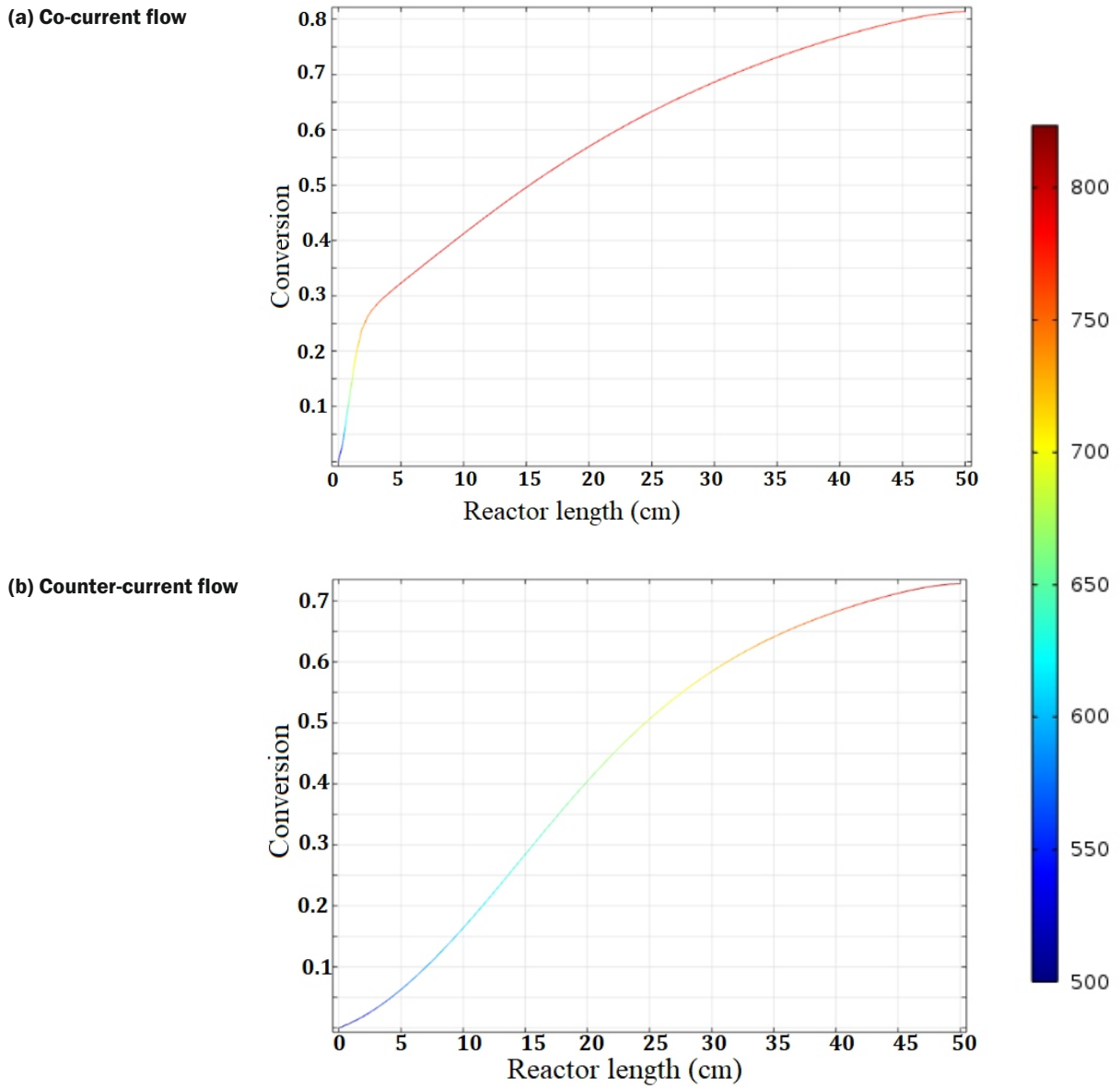

Fig.13: Effect of flow patterns on conversion of HI (T_1 = 773 K, T_i= 500K, x_{10} = 0.95, ε = 0.3, p_0 = 303975 Pa, u_0 = 0.0005 m/s).

compared to a conversion of ~73% in counter-current flow. This is because in co-current flow, there is a higher temperature near the inlet of the reactor (where concentration of HI is higher) which leads to enhanced reaction rate and conversion increases. This can also be seen in the curve (Fig.13(a)), in which the temperature of gas mixture remains higher at the inlet of the reactor, in case of co-current flow. For counter-current flow, since the molten salt enters from opposite end, the HI in the feed remains at a lower temperature (as can be seen in curve in Fig.13(b)) which leads to a lower overall conversion. Similar trend can be seen in temperature contours shown in Fig.14. Fig.15 shows the mole fraction of HI inside the membrane reactor for both the flow patterns. It can be seen that in case of co-current flow the mole fraction of HI is lower inside the membrane reactor as compared to counter-current flow due to reasons already mentioned above.

Effect of outer radius of membrane tube

Fig.16 shows that there is an increase in conversion as outer radius of membrane tube increases. The conversion increases from 64% to 83% on increasing membrane tube radius from 1.8 cm to 3.6 cm. This is because of increased membrane surface area and hence increase in hydrogen permeation due to increase in outer radius. As the targeted conversion is 80%, the optimum outer radius in this case will be 3.6 cm.

Optimum parameters for molten salt heated membrane reactor

A final simulation was carried out using packed bed configuration of a membrane reactor taking into account various considerations and results obtained as mentioned in previous sections, with following parameters:

- Feed velocity = 0.0005 m/s
- Molten salt inlet temperature = 773 K
- Outlet pressure = 3 bar
- Membrane tube outer radius = 3.6 cm
- Reactor length = 50 cm
- Feed temperature = 500 K
- Feed Composition: 95% HI
- Packed bed porosity = 0.3

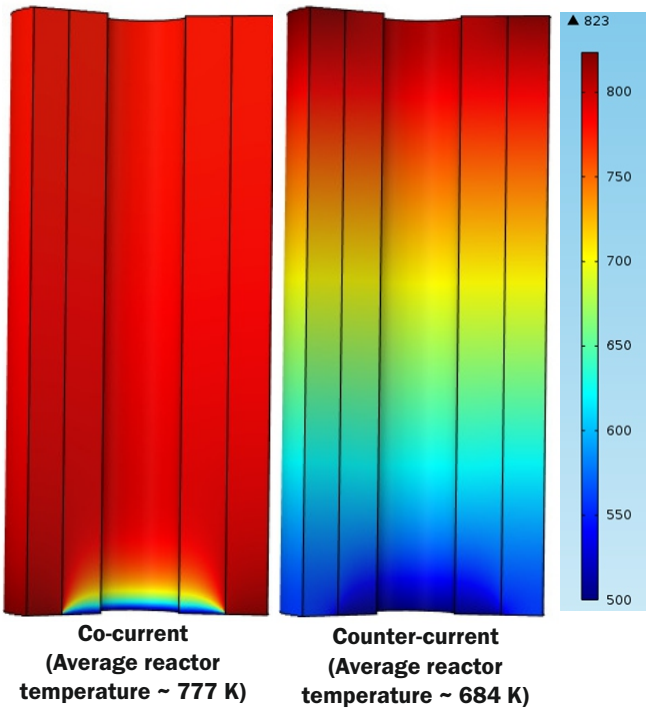

Fig.14: Contours of temperature inside the membrane reactor for co-current and counter-current flow (T_1 = 773 K, T_f = 500K, x_{10} = 0.95, ε = 0.3, p_0 = 303975 Pa, u_0 = 0.0005 m/s).

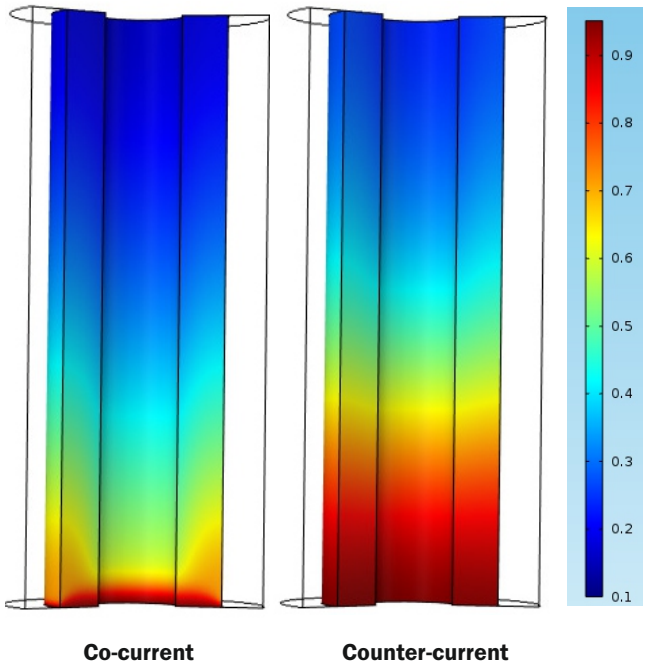

Fig.15: HI mole fraction profile inside the membrane reactor for co-current and counter-current flow (T_1 = 773 K, T_f = 500K, x_{10} = 0.95, ε = 0.3, p_0 = 303975 Pa, u_0 = 0.0005 m/s).

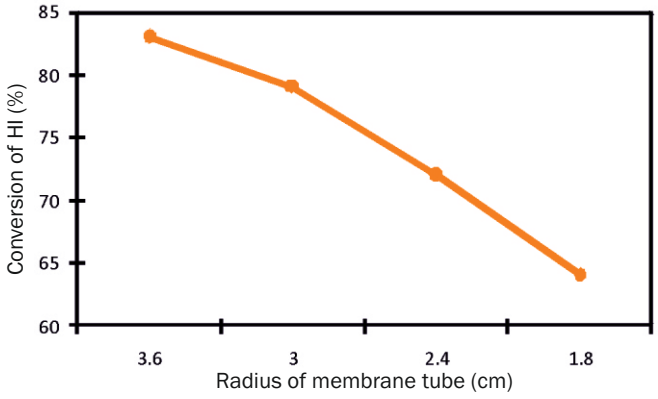

Fig.16: Effect of membrane tube radius on conversion of HI (T_1 = 773 K, T_f = 500K, x_{10} = 0.95, ε = 0.3, p_0 = 3,03,975 Pa, u_0 = 0.0005 m/s).

The conversion obtained for simulation of this design was 83%. The contours of mole fractions of HI, H_2 and I_2 for this simulation are shown in Fig.17. The hydrogen mole fraction first increases near the inlet and then decreases to become constant near the outlet. This is because near the inlet, hydrogen is produced due to HI decomposition and it permeates out from the membrane throughout the reactor length and its mole fraction decreases. The mole fraction of iodine increases along the reactor length as it is produced by reaction, with a higher mole fraction near the walls where hydrogen permeates out. It becomes constant near the outlet confirming that the entire reactor length as well the membrane surface area is sufficient to achieve the maximum conversion possible in this configuration.

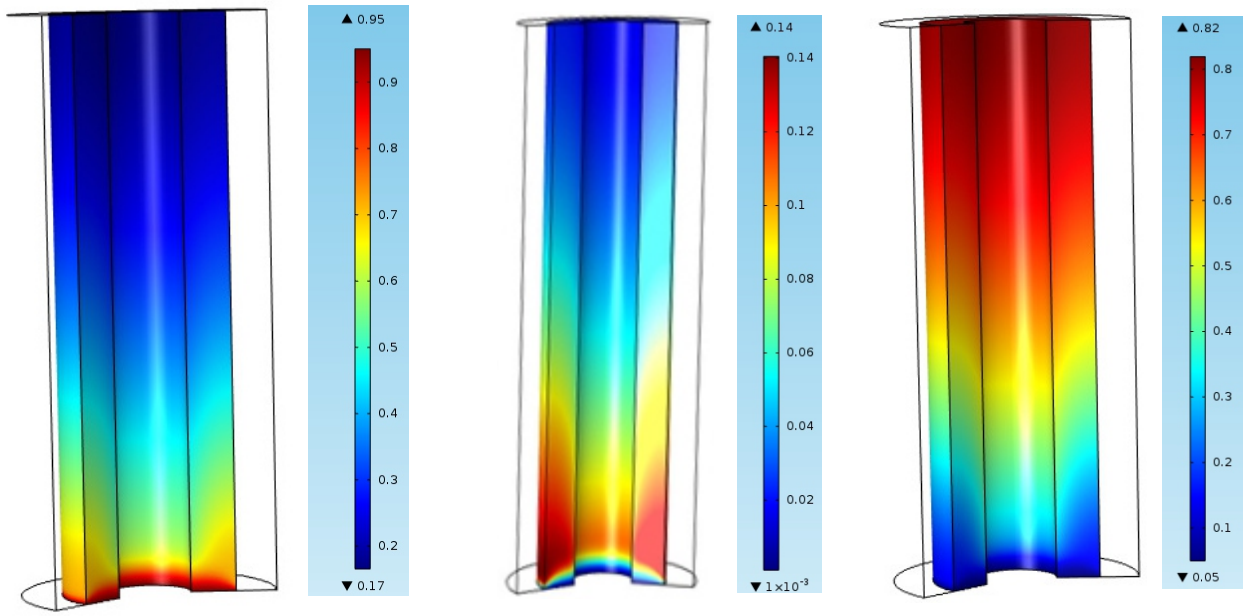

Fig.17: Contours of mole fraction of HI, H_2 and I_2 inside the membrane reactor at optimum parameters.

Conclusions

A CFD model of molten salt heated packed bed membrane reactor for HI decomposition is reported. The computational approach used in the model was validated with the literature data. Subsequently, the validated model was used for parametric analysis which provides important insights into the effect of various operating conditions on the performance of membrane reactor for HI decomposition reaction. The optimum molten salt inlet temperature was found to be ~773 K because as the temperature increases further, it has minimal effect on the conversion, while posing materials challenges. With increase in pressure, the conversion was found to increase. It was found that co-current flow of molten salt with respect to feed flow gives a higher conversion as compared to counter-current flow. The optimum parameters were found to be: feed velocity = 0.0005 m/s; molten salt inlet temperature = 773 K; outlet pressure = 3 bar; membrane tube outer radius = 3.6 cm; reactor length = 50 cm. A conversion of ~83% was achieved with these parameters at a HI throughput of ~ 400 ml/min. It was found that membrane reactor enhanced the conversion at least by ~ 60% above & beyond that obtained in a conventional packed bed reactor. The CFD model embedding all the transport phenomena, reported in this study can be used as a virtual prototyping tool to screen potential design alternatives.

Acknowledgements

The authors acknowledge the requisite COMSOL computing support and technical guidance provided by Dr. K.K. Singh, Chemical Engineering Division (ChED), BARC.

References

[1] J. E. Murphy, J. P. O'Connell, "Process simulations of HI decomposition via reactive distillation in the sulfur-iodine cycle for hydrogen manufacture", Int. J. Hydrog. Energy, 37 (2012), pp 4002-4011.

[2] T. D.B. Nguyen, Y-K. Gho, W. C. Cho, K. S. Kang, S. U. Jeong, C. H. Kim, C-S. Park, K-K. Bae, "Kinetics and modeling of hydrogen iodide decomposition for a bench-scale sulfur–iodine cycle", Appl. Energy, 115 (2014) 531–539.

[3] S. Kar, R.C. Bindal, S. Prabhakar, P.K. Tewari, "The application of membrane reactor technology in hydrogen production using S-I thermochemical process: A roadmap", Int. J. Hydrog. Energy, 37 (2012), pp 3612-3620.

[4] O. Yoshinao, K. Toshiya, M. Susumu, K. Wakichi, T. Yoshio, F. Kinjiro, "Kinetics of the catalytic decomposition of hydrogen iodide in the magnesium-iodine thermochemical cycle", Bull. Chem. Soc. Jpn., 54 (1981), pp 742-748.

[5] G.-J. Hwang, K. Onuki, "Simulation study on the catalytic decomposition of hydrogen iodide in a membrane reactor with a silica membrane for the thermochemical water-splitting IS process", J. Membr. Sci., 194 (2001), pp 207-215.

[6] JANAF Thermochemical Tables, Dow Chemical Company, Midland, 1977.

[7] N. Goswami, K.K. Singh, S. Kar, R.C. Bindal, P.K. Tewari, Numerical simulations of HI decomposition in packed bed membrane reactors, Int. J. Hydrog. Energy, 39 (2014), pp 18182-18193.

[8] A. Karim, J. Bravo, A. Datye, Non isothermality in packed bed reactors for steam reforming of methanol, Appl. Catal. A: General, 282 (2005), pp 101–109.

Notations

A	area of reactor wall	(m^2)
C_p	effective heat capacity of gas mixture	(J/mol.K)
d_p	particle diameter	(m)
D_{ij}	binary diffusivity	(m^2/s)
D_i	Diffusivity of i^{th} species	(m^2/s)
ΔG	change in Gibbs free energy	(kJ/mol)
k	rate constant	(mol m^{-3} Pa^{-1} s^{-1})
k_t	effective thermal conductivity	(W/m.K)
K_{I2}	adsorption equilibrium constant of iodine	(Pa^{-1})
K_p	equilibrium constant	
p	pressure	(Pa)
p_0	pressure at outlet of reactor	(Pa)
Pe	permeance of membrane for hydrogen	(mol/m^2.Pa.s)
Q	heat source	(W/m^3)
Q_w	heat transferred to reaction zone through reactor wall	(W/m^3)
r_{HI}	rate of reaction	(mol m^{-3} s^{-1})
R	universal gas constant	(J/mol.K)
R_i	source term due to reaction for species	(kg/m^2.s)
t	time	(s)
T	temperature of gaseous mixture	(K)
T_f	feed temperature	(K)
T_1	molten salt inlet temperature	(K)
T_2	temperature of molten salt	(K)
$\vec{u}$	velocity vector	(m/s)
u_0	magnitude of x component of feed velocity	(m/s)
U	overall heat transfer coefficient	(W/m^2. K)
x_j	mole fraction of component j	(j=1 (HI), 2 (H_2), 3 (I_2))
x_{j0}	mole fraction of component j at reactor inlet	(j=1 (HI), 2 (H_2), 3 (I_2))

Symbols

κ	hydraulic permeability of porous medium	(m^2)
ϕ_e	equilibrium conversion	(~0.21 at 700 K)
ω_j	mass fraction of component j	
η	viscosity of the gaseous mixture	(kg/m.s)
ε	porosity of bed	
ρ	effective density of gas mixture	(kg/m^3)